

# Abrupt Early to Mid-Holocene Climatic Transition Registered at the Equator and the Poles

J. C. Stager\* and P. A. Mayewski

Paleoclimatic records from equatorial East Africa, Antarctica, and Greenland reveal that atmospheric circulation changed abruptly at the early to mid-Holocene transition to full postglacial conditions. A climatic reorganization occurred at all three sites between 8200 and 7800 years ago that lasted 200 years or less and appears to have been related to abrupt transitions in both marine and terrestrial records around the world.

Late Pleistocene climates fluctuated dramatically on decadal to century scales (1, 2). Recent high-resolution records have shown that the warmer Holocene, though relatively more stable than the late Pleistocene, was also subject to rapid change (3–7). Climatic instability during warm interglacials has important implications for the modeling of anthropogenic effects on modern climates. Here we examine the timing of the Holocene climatic reorganization that was associated with the final retreat of large continental ice sheets and the resultant stabilization of global sea levels around 8000 years ago (8, 9) [all dates are given in calendar years before the present (B.P.) (2000 A.D.); the conversions are after (10)]. In this early to mid-Holocene transition (EMHT), the summer monsoons weakened over the western Indian Ocean (3), tropical precipitation declined or became more seasonal (11–13), and precipitation changed at mid-latitude sites (4, 11, 14).

The timing and distribution of the EMHT have been uncertain, which makes it difficult to evaluate causal mechanisms. To address these questions, we compared records of the EMHT in paleoclimate records from the equator and both poles (Fig. 1). We examine a fine-interval diatom record from northern Lake Victoria, East Africa (0°05'0"N, 32°48'2"E) (7), Greenland's Greenland Ice Sheet Project Two (GISP2) ice core record (72.6°N, 38.5°W) (5), and a new Holocene ice core record from Taylor Dome (TD), East Antarctica (77°47.7'S, 158°43.1'E). The temporal resolution was ~200 years at GISP2 (15) and somewhat greater at TD and Lake Victoria.

The Lake Victoria diatom record (30- to 45-year intervals) was obtained from core Ibis-1 from the Damba Channel (Fig. 1) and is calibrated with three bulk <sup>14</sup>C dates that vary linearly with depth over the past ~13,000 years. More abundant dates in

other cores also show that middle and late Holocene sedimentation at Lake Victoria was relatively steady (16, 17). We used a <sup>14</sup>C reservoir correction of 600 years, which is the approximate <sup>14</sup>C age of recent sediments and is consistent with linear extrapolation of surface sediment ages in two cores (7, 17–19).

Correspondence analysis ordination (CA) [which is similar to principal components analysis (20)] of the diatom series summarizes Holocene limnological changes in northern Lake Victoria (Figs. 2 and 3). The first axis [CA1 (Fig. 3)] tracks the abundances of *Aulacoseira nyassensis* and *Nitzschia fonticola* (Fig. 2), which are thought to reflect seasonal wind-driven mixing and stratification, respectively, in Lake Victoria (7). Increased seasonality of mixing favors *A. nyassensis* over other *Aulacoseira* species that are less capable of surviving prolonged stratification episodes (7, 21). We thus use CA1 as a proxy for the degree of wind-driven mixing. The second axis [CA2 (Fig. 3)] is correlated with the abundances of *A. granulata* and *A. ambigua* (Fig. 2) and appears to be a proxy of precipitation: evaporation ratios (P:E) or lake depth (7).

The GISP2 chronology (which uses smoothed 2-year intervals) is based on annual layer counts (15, 22). The TD chronology (which uses 25-year intervals) is based on ice flow modeling, marker horizons, and isotopic correlations with other Antarctic ice cores (23). High sodium (Na) concentrations in the two cores (Fig. 3) are thought to reflect intensified meridional circulation and atmospheric mixing. The Na is derived primarily from oceans at lower latitudes (5, 24).

High northern summer insolation during the early Holocene strengthened monsoons and contributed to warm, humid conditions throughout the tropics (11–13). Northern Lake Victoria was well mixed by frequent strong winds, and P:E or lake levels were high, with a peak in CA2 developing between 8200 and 7800 years B.P. (Figs. 2 and 3). Sodium deposition declined rapidly at GISP2 and TD with post-Pleistocene

warming and weakening of polar atmospheric circulation (2), which leveled off at ~10,300 years B.P. (Fig. 3).

A century-scale, globally distributed cooling event (5, 25) corresponds with a Na peak in both the TD and GISP2 records (26) between 8400 and 8200 years B.P. (Fig. 3). There was a decline in P:E or depth at Lake Victoria around 8300 to 8200 years B.P. (Fig. 3) that was more strongly developed at several tropical African sites (12) and may have been related to the polar cooling event.

Shortly after ~8200 years B.P., Na concentrations declined sharply at GISP2 and at TD during the CA2 peak at Lake Victoria (Fig. 3). At ~7800 years B.P., Na concentrations declined at TD and at GISP2, whereas microfossil changes in Ibis-1 and other cores imply that both P:E and wind activity decreased rapidly at Lake Victoria (7, 16, 17) (Fig. 2). We interpret the changes close to 8200 (GISP2) and 7800 years B.P. (TD and Lake Victoria) to represent the EMHT at these three sites. Our data indicate that these shifts lasted 200 years or less.

After 7800 years B.P., Na concentrations recovered quickly at GISP2 and fluctuated throughout the remainder of the Holocene. In contrast, the EMHT evidently altered climates profoundly at Lake Victoria and TD. Aridity or rainfall seasonality (or both) increased throughout much of the tropics after the EMHT (12, 13, 27), and the seasonality of rainfall and lake mixing increased rapidly at Lake Victoria core sites (7, 16, 17) (Figs. 2 and 3). Rainfall seasonality also increased abruptly in much of North Africa at ~7800 years B.P. (28). Although P:E rose at ~6500 years B.P. at many tropical African sites (12), Lake Victoria's CA2 declined from the EMHT to

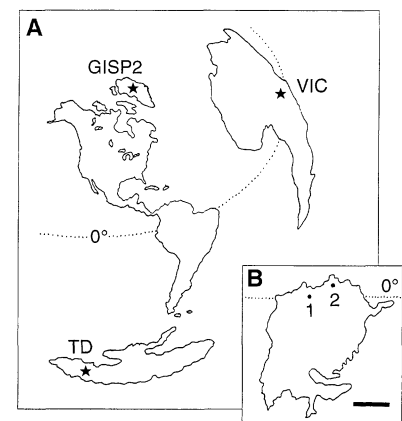


**Fig. 1.** (A) Locations of GISP2, Lake Victoria (VIC), and TD core sites. (B) Lake Victoria with Damba Channel (1) and Pilkington Bay (2) core sites; scale bar, 100 km.

Climate Change Research Center, Institute for the Study of Earth, Oceans and Space, University of New Hampshire, Durham, NH 03824, USA.

\*To whom correspondence should be addressed at Math/Science Division, Paul Smith's College, Paul Smiths, NY 12970, USA. E-mail: stagerj@paulsmiths.edu

the present in response to decreasing P:E and downcutting of the Nile outlet (7) (Fig. 3). At TD, Na concentrations remained low for ~2000 years after the EMHT and only recovered slowly after 5500 years B.P. The drop in Na influx at TD may reflect diminution of meridional circulation,

which is possibly related to a decline in the extent of Antarctic sea ice (29) [which also occurred in the Arctic Ocean (9)] that might have shifted circumpolar air masses poleward. Dust production declined and P:E increased at middle latitudes on the southern continents (12–14).

Our data suggest that the climatic changes associated with the EMHT occurred simultaneously in Africa and Antarctica but may have begun somewhat earlier in Greenland, although the degree of difference is within the dating errors for these records.

Other prominent examples of century-scale climatic reorganizations at ~8000 to 7500 years B.P. have been seen in records from around the world, including records from North America (30), the North Atlantic Ocean, the Arabian and Caribbean Seas (3, 31), and Asia (32). An unusual “triple oscillation” (a rapid sequence of Maunder and Spörer-type disturbances) occurred in the atmospheric <sup>14</sup>C record from 8400 to 7800 years B.P. (33). Thus, the EMHT may have been associated with disruptions of ocean circulation or a change in solar radiance or cosmic ray flux.

Our results show that at least one climatic change during the Holocene was widely distributed and abrupt in both the tropics and the southern regions. Furthermore, the Holocene paleoclimatic record of northern Lake Victoria, which is located at the equator, more closely resembles the Antarctic record than that of Greenland. This comparison supports recent models linking Holocene climatic fluctuations in tropical and southern Africa (14, 34) and South America (13) to changes in Antarctic weather systems and circumpolar ocean currents.

**Fig. 2.** Holocene microfossil records from Lake Victoria. Pollen records of seasonally dry *Celtis* and moister Moraceae-rich forests from Pilkington Bay are shown. [28 <sup>14</sup>C dates (16)]. Selected diatom series from the Damba Channel core are primary bases for the CA axes discussed in the text. *Aulacoseira granulata* and *A. ambigua* indicate well-mixed conditions; benthic *Fragilaria* reflect low lake levels and increased mixing. EMHT, early mid-Holocene transition at 8200 to 7800 years B.P.

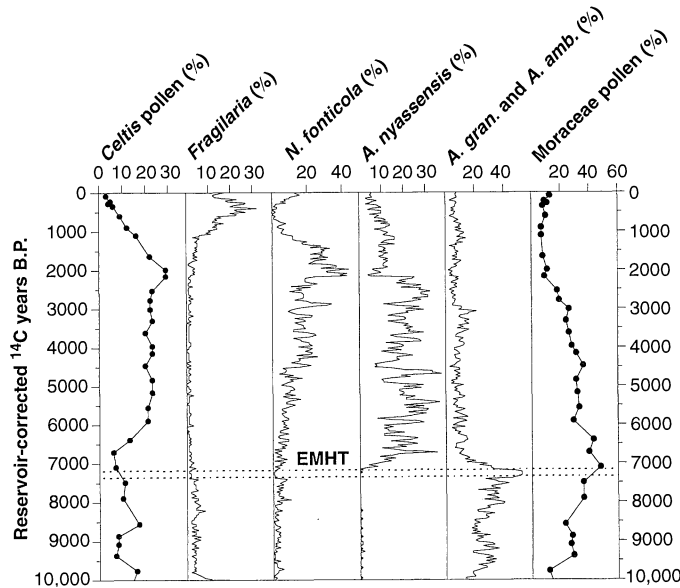
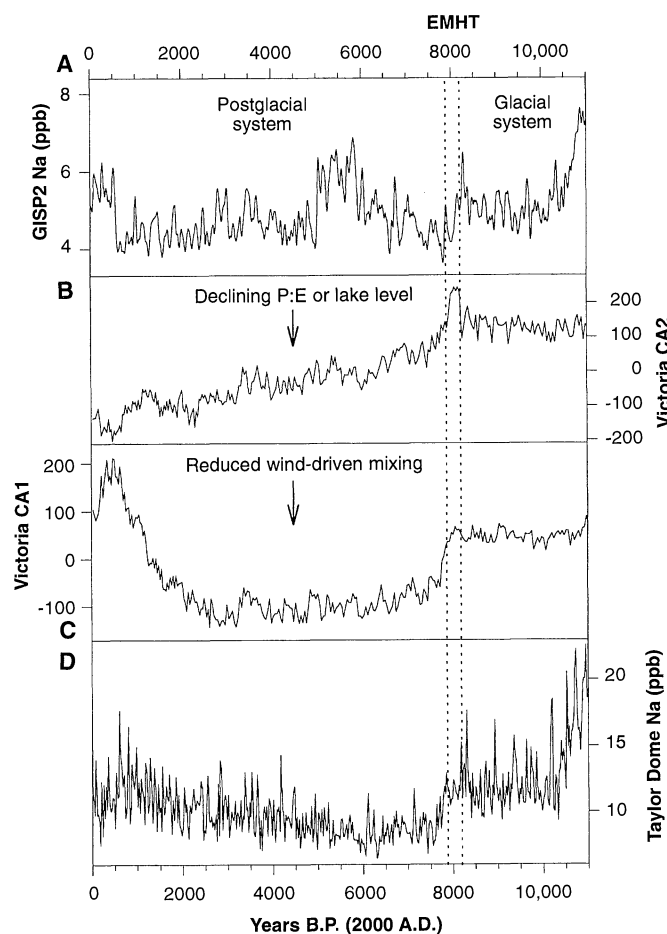


**Fig. 3.** Holocene chemical and microfossil records from the equator and poles. Sodium at GISP2 (A) and TD (D) represents the strength of meridional transport and atmospheric mixing. Lake Victoria CA1 (C) and CA2 (B) represent wind-driven mixing and P:E or lake depth, respectively.



REFERENCES AND NOTES

1. W. Dansgaard *et al.*, *Nature* **364**, 218 (1993); J. W. C. White, *ibid.*, p. 186.
2. P. A. Mayewski *et al.*, *Science* **261**, 195 (1993).
3. F. Sirocko *et al.*, *Nature* **364**, 322 (1993).
4. H. F. Lamb *et al.*, *ibid.* **373**, 134 (1995); J. T. Overpeck, *Science* **271**, 1820 (1996).
5. S. R. O'Brien *et al.*, *Science* **270**, 1962 (1995).
6. K. R. Laird, S. C. Fritz, E. C. Grimm, P. G. Mueller, *Limnol. Oceanogr.* **41**, 890 (1996).
7. J. C. Stager, B. Cumming, L. D. Meeker, *Quat. Res.* **47**, 81 (1997).
8. M. Nakada and K. Lambeck, *Nature* **333**, 36 (1988).
9. R. Stein *et al.*, *Science* **264**, 692 (1994).
10. E. Bard, M. Arnold, R. G. Fairbanks, B. Hamelin, *Radiocarbon* **35**, 191 (1993); M. Stuiver and P. J. Reimer, *ibid.*, p. 215.
11. COHMAP Members, *Science* **241**, 1043 (1988).
12. S. E. Nicholson and H. Flohn, *Clim. Change* **2**, 313 (1980); F. A. Street-Perrott and N. Roberts, in *Variations in the Global Water Budget*, F. A. Street-Perrott *et al.*, Eds. (Reidel, Norwell, MA, 1983), pp. 331–345.
13. M. Servant *et al.*, *Global Planet. Change* **7**, 25 (1993).
14. T. C. Partridge, *Palaeogeogr. Palaeoclimatol. Palaeoecol.* **101**, 237 (1993).
15. R. B. Alley *et al.*, *Nature* **362**, 527 (1993).
16. R. L. Kendall, *Ecol. Monogr.* **39**, 121 (1969). The pollen record of Pilkington Bay core P-2 (see text) has 28 bulk <sup>14</sup>C dates.
17. T. C. Johnson *et al.*, *Science* **273**, 1091 (1996); J. C. Stager and T. J. Johnson, in preparation. The diatom record of offshore core V95-2P has nine accelerator mass spectrometer dates.
18. M. Stuiver, in *Radiocarbon Variations and Absolute Chronology*, I. U. Olsson, Ed. (Wiley, New York, 1970), pp. 197–213.
19. R. E. Hecky, *Verh. Int. Verein. Limnol.* **25**, 39 (1993).

20. C. J. F. Ter Braak, *Technical Report LWA-88-02* (Institute of Applied Computer Science, Wageningen, Netherlands, 1988).
21. J. F. Talling, *Int. Rev. Ges. Hydrobiol.* **51**, 545 (1966); P. Kilham, S. S. Kilham, R. E. Hecky, *Limnol. Oceanogr.* **31**, 1169 (1986).
22. D. Meese *et al.*, *U.S. Army Cold Reg. Res. Eng. Lab. Publ. SR94-01* (1994).
23. P. M. Grootes *et al.*, *Eos* **75**, 225 (1994); P. A. Mayewski *et al.*, *Science* **272**, 1636 (1996).
24. P. A. Mayewski *et al.*, *Science* **263**, 1747 (1994).
25. T. M. L. Wigley, in *Global Changes of the Past*, R. S. Bradley, Ed. (University Consortium of Atmospheric Research, Office for Interdisciplinary Earth Studies, Boulder, CO, 1989), pp. 83–101.
26. R. B. Alley *et al.*, *Geology*, in press.
27. R. B. Owen, J. W. Barthelme, R. W. Renaut, A. Vincens, *Nature* **298**, 523 (1982); K. W. Butzer, G. L. Isaac, J. L. Richardson, C. Washbourn-Kamau, *Science* **175**, 1069 (1972).
28. J. Maley, *Quat. Res.* **18**, 1 (1982).
29. P. A. Mayewski *et al.*, *Antarct. Res. Ser.* **67**, 33 (1995).
30. D. A. Fisher, R. M. Koerner, N. Reeth, *Holocene* **5**, 19 (1995); X. Feng and S. Epstein, *Science* **265**, 1079 (1994); R. W. Mathewes and L. E. Heusser, *Can. J. Bot.* **59**, 707 (1981).
31. P. Blanchon and J. Shaw, *Geology* **23**, 4 (1995); J. T. Overpeck *et al.*, *Nature* **338**, 553 (1989).
32. E. van Campo and F. Gasse, *Quat. Res.* **39**, 300 (1993); A. Frumkin *et al.*, *Holocene* **1**, 191 (1991); R. A. Bryson and A. M. Swain, *Quat. Res.* **16**, 135 (1981).
33. M. Stuiver and T. F. Brauzanias, *Nature* **338**, 405 (1989).
34. P. D. Tyson and J. A. Lindesay, *Holocene* **2**, 271 (1992); T. C. Partridge, *Mem. Soc. Geol. France* **167**, 73 (1995).
35. We thank the NSF for financial support for the TD ice core project; the Polar Ice Coring Office (University of Alaska) drillers, notably D. Giles; the Antarctic Support Associates personnel for camp support and logistics; Squadron VXE6 and the New York Air National Guard (TAG 109) for air support; P. Grootes, E. Steig, M. Stuiver, D. Morse, E. Waddington, and other colleagues at the University of Washington for organizing, collecting, and dating the TD ice core; and K. Beuning, B. Cumming, S. Grimm, T. Johnson, K. Laird, D. Livingstone, M. Martin, L. Meeker, Paul Smith's College, and J. Smol for support in the Lake Victoria project.

25 February 1997; accepted 25 April 1997

## Giant Planet Formation by Gravitational Instability

Alan P. Boss

The recent discoveries of extrasolar giant planets, coupled with refined models of the compositions of Jupiter and Saturn, prompt a reexamination of theories of giant planet formation. An alternative to the favored core accretion hypothesis is examined here; gravitational instability in the outer solar nebula leading to giant planet formation. Three-dimensional hydrodynamic calculations of protoplanetary disks show that giant gaseous protoplanets can form with locally isothermal or adiabatic disk thermodynamics. Gravitational instability appears to be capable of forming giant planets with modest cores of ice and rock faster than the core accretion mechanism can.

The discovery of extrasolar giant planets (1–5) presents theorists with the challenge of trying to understand the formation of these planets within the context of the generally accepted core accretion model for the formation of the solar system's giant planets. The core accretion model envisions the formation of cores of roughly  $10 M_{\oplus}$  ( $M_{\oplus}$  = the mass of Earth) through planetesimal collisions, followed by rapid accretion of gas from the solar nebula (6). However, the core accretion model suffers from the fact that the time needed to assemble the  $10 M_{\oplus}$  cores, which is on the order of  $10^6$  years in the most optimistic scenario (7), lies in the middle of the range of ages ( $\sim 10^5$  to  $\sim 10^7$  years) at which young solar-type stars lose their gaseous disks (8). If the disk gas has already dissipated by the time that  $10 M_{\oplus}$  cores form, then Uranus-like planets would result, rather than Jupiter-like planets, a fate that led to some understandable pessimism about the frequency of occurrence of extrasolar giant planets (9).

The detection of a number of extrasolar planets with minimum masses ranging from 0.5 to  $4 M_J$  ( $M_J = 318 M_{\oplus}$  = the mass of Jupiter) has removed much of the concern that giant planets might be rare in our

galaxy. For detection by the radial velocity technique, the planet's mass will be considerably larger than the minimum if the planet's orbit is nearly in the plane of the sky. The suspected giant planets orbiting 47 Ursae Majoris (2), Lalande 21185 (3), and 16 Cygni B (4) have semimajor axes of 2 to 7 astronomical units (AU) ( $1 \text{ AU} = 1.5 \times 10^{13} \text{ cm}$  = the distance from Earth to the sun), and have minimum masses of 1.5 to  $2.4 M_J$ ; Lalande 21185's astrometrically detected planet is fixed in mass at  $1.5 M_J$ . The core accretion model may be unable to produce giant planets more massive than about  $1 M_J$  if the growing planet's gravity induces a gap in the surrounding disk (10). In addition, suspected brown dwarf stars (stars with  $M < 80 M_J$ ) have also been found in orbit around nearby stars (11), with minimum masses as small as  $6.6 M_J$  (12), possibly blurring any mass-based distinction between planets and brown dwarf stars (13).

The core accretion model won favor largely because of its ability to explain the similarity of the masses of the ice and rock cores inferred for Jupiter, Saturn, Uranus, and Neptune through the prediction (14) of the existence of a single critical core mass ( $\sim 10 M_{\oplus}$ ) that would trigger gas accretion throughout the solar nebula. However, recent models of the interior

structure of Jupiter and Saturn (15) have concluded that their ice and rock core masses are smaller than had previously been thought likely: 3 to  $10 M_{\oplus}$  for Jupiter and 1 to  $13 M_{\oplus}$  for Saturn, as compared with the older estimates (16) of 10 to  $30 M_{\oplus}$  for Jupiter and 15 to  $25 M_{\oplus}$  for Saturn. If the lower estimates are accurate, then much of the attraction of the core accretion theory would be lost because lower mass cores might not be able to trigger gas accretion.

For these and other reasons (7), it seems prudent to reevaluate the possible mechanisms for giant planet formation. One hypothesis is the gravitational instability mechanism (17), in which the solar nebula breaks up through its own self-gravity into clumps of gas and dust, termed giant gaseous protoplanets (GGPPs), which then contract and collapse to form giant planets (18). The GGPP mechanism was discarded because of its failure to explain the large values and similarity of estimated core masses for both the giant and the outer planets (6, 16), but these problems may no longer exist.

Previous work on gravitational instabilities in disks had suggested that marginally unstable disks would evolve through the formation of spiral density waves (19), thereby avoiding GGPP formation, and that GGPPs could only occur if the disks were strongly unstable (20). GGPP formation also seemed to require that the instability proceed at a fixed temperature at a given orbital radius (that is, locally isothermal), in order to prevent thermal pressure from damping the growth of the perturbations (20).

In the process of calculating axisymmetric models of the temperature distribution in the solar nebula (21), the general trend arose of relatively hot (midplane temperature  $T_m \sim 1000 \text{ K}$ ) regions inside a few AU, surrounded by relatively cold ( $T_m \sim 100 \text{ K}$ ) outer regions. In disks with masses of  $\sim 100 M_J$  inside 10 AU, the outer regions were dense enough to be

Department of Terrestrial Magnetism, Carnegie Institution of Washington, Washington, DC 20015–1305, USA.